ICARUS-TM-97/18
15 December 1997

Simulation of Nuclear Effects in neutrino interactions

D. Cavalli*, A. Ferrari*and P.R. Sala*

* INFN, Sezione di Milano

1 Introduction

The final state kinematics in a neutrino-nucleus interaction is in principle different from the free neutrino-nucleon one. The extent of this difference has never been investigated in details, although it can heavily affect the results of present and future neutrino experiments.

Nuclear effects include initial state effects, essentially related to nucleon Fermi motion, and final state effects, due to reinteractions of the scattered hadrons in the nucleus, to deflections in the nuclear and Coulomb fields, and to reaction Q-values.

All these factors have been taken into account in the calculations presented in this note, by exploiting the nuclear interaction model already developed for the FLUKA code [1, 2, 3, 4, 5].

Since no neutrino interaction generator was available in FLUKA when calculations were performed, [1] both Charged and Neutral current events from free neutrino-nucleon interactions have been generated using external codes[6] and used as source for FLUKA . Comparisons of the free and the bound final states have been performed for quasielastic interactions and interactions with Δ^+ and Δ^{++} resonance production.

2 FLUKA nuclear model

Descriptions of FLUKA and its developments can be found in [1, 2, 3, 5]. Here only those parts relevant to the present investigation are described, that is the nuclear interaction generator, and more precisely the intermediate energy model, called PEANUT . A thourough description of the nuclear interaction models, together with several comparisons with experimental data can be found in [5].

2.1 General structure

Presently, PEANUT handles interactions of nucleons, pions, kaons, and γ rays from about 3 GeV down to reaction threshold (or 20 MeV for neutrons). Other models are used in FLUKA for higher energies, the main difference being their simplified treatment of nuclear effects. The approach of PEANUT is going to be progressively extended to higher energies, borrowing from the high energy models the description of hadron-nucleon interactions and inserting them into the complex nuclear framework of PEANUT .

The reaction mechanism is modelled in PEANUT by explicit intranuclear cascade (INC) smoothly joined to statistical (exciton) preequilibrium emission [7, 8].

[1] A model for QuasiElastic ν - nucleon interactions is now implemented in FLUKA and can be used directly within the FLUKA nuclear interaction generator, removing the need for external event generators. Both Charged and Neutral Current processes are considered, the outgoing lepton mass is taken into account and its polarization is computed.

At the end of the INC and exciton chain, the evaporation of nucleons and light fragments (α, d, ^{3}H, ^{3}He) is performed, following the Weisskopf [9] treatment. Care has been taken in adopting suitable forms for the nuclear level density and the inverse cross sections [10]. Competition of fission with evaporation has been implemented, again within a statistical approach.

Since the statistical evaporation model becomes less sound in light nuclei, the so called Fermi Break-up model [11, 12] is used instead. The excited nucleus is supposed to disassemble just in one step into two or more fragments, with branching given by plain phase space considerations.

The excitation energy still remaining after (multiple) evaporation is dissipated via emission of γ rays [13].

2.2 INC generalities

The INC proceeds through hadron multiple collisions in a cold Fermi gas. The hadron-nucleon cross sections used in the calculations are free hadron-nucleon cross sections. The Fermi motion is taken into account when considering elementary collisions, both for the purpose of computing the interaction cross section, and to produce the final state particles.

Secondaries are treated exactly like primary particles, with the only difference that they start their trajectory already inside the nucleus. Primary and secondary particles are transported according to their nuclear mean field and to the Coulomb potential. All particle are transported along classical trajectories, nevertheless a few relevant quantistic effects are included.

Binding Energies (B_{en}) are obtained from mass tables, depending on particle type and on the actual composite nucleus, which may differ from the initial one in case of multiple particle emission. Relativistic kinematics is applied, with accurate conservation of energy and momentum, and with inclusion of the recoil energy and momentum of the residual nucleus.

2.3 Nuclear geometry

In both stages, INC and exciton, the nucleus is modelled as a sphere with density given by a symmetrized Woods-Saxon [14] shape for A>16,

$$\begin{aligned} \rho(r) &= \rho_0 \frac{\sinh(\mathrm{R_0/a})}{\cosh(\mathrm{r/a}) + \cosh(\mathrm{R_0/a})} \\ &\approx \frac{\bar{\rho}_0}{1 + \exp\frac{r - R_0}{a}} \end{aligned} \tag{1}$$

and by a harmonic oscillator shell model for light isotopes (see [15]). It is radially divided in 16 zones of constant density, and its boundary is set at the radius (R_{nuc}) where the density is one hundredth of the central one. Six radial zones are added to allow a suitable description of the nuclear potential ouside the nucleus, and finally 10 extra radial bins are there for charged particles to describe the long range effect of the Coulomb potential.

Proton and neutron densities are generally different, according again to shell model ones for A<16, and to the droplet model [16, 17] for heavier nuclei.

2.4 Fermi motion and Nuclear Potential

A standard position dependent Fermi momentum distribution is implemented in PEANUT :

$$\frac{\mathrm{dN}}{dk} = \frac{|k|^2}{2\pi^2} \tag{2}$$

for k up to a local Fermi momentum $k_F(r)$ given by

$$k_F(r) = \left(\frac{3\pi^2}{2}\rho(r)\right)^{\frac{1}{3}} \tag{3}$$

where ρ is the neutron or proton density as defined in the previous paragraph.

The potential depth felt by nucleons at any radius r is given by the Fermi kinetic energy plus the relevant binding energy.

Work is in progress to implement high momentum tails in the nucleon momentum distribution [18, 19]. According to the literature, these tails should affect about 10% of the nucleons, and they should reflect in the final kinematics as events with some extra unbalance in the hadron-lepton system. Since, however, the nuclear spectral function for high momenta is centered at high removal energies, we espect that interactions on high momentum nucleons will be strongly Pauli suppressed and will result in low energy outgoing protons. As will be described later, already a standard Fermi momentum distribution when included in a complete framework produces similar tails in the momentum distribution. For pions, a nuclear potential has been calculated starting from the standard pion-nucleus optical potential [24].

2.5 Cross sections

2.5.1 Nucleon-nucleon

Nucleon-nucleon total cross sections, both elastic and inelastic, are taken from available experimental data. Elastic scattering is explicitly performed according to the experimental differential cross sections.

Pion production is the first inelastic channel to be open both in pion-nucleon and nucleon-nucleon interactions, obviously because of the small pion mass. The reaction $N_1 + N_2 \to N_1' + N_2' + \pi$ has its threshold around 290 MeV, and it starts to be important around 700, while the reaction $\pi + N \to \pi' + \pi'' + N'$ opens at 170 MeV. The dominance of the Δ resonance, and of the N^* resonances at higher energies, in the π, N channel suggest to treat both reactions in the framework of the isobar model, that is to assume that they all proceed through an intermediate state containing at least one resonance. In the intermediate state the resonance can be treated as a real particle, that is, in a Monte Carlo code it can be transported and then transformed into secondaries according to its lifetime and decay branching ratios.

The isobar model accommodates easily multiple pion production, simply allowing the presence of more than one resonance in the intermediate state. These processes are simulated in PEANUT by coupling the resonance production part of the HADRIN [20] code, suitably modified, to all the subsequent intranuclear steps. The relative resonance decay branching ratio in different pion and nucleon charge states have been computed through isospin relations.

2.5.2 Pion-nucleon

Pion induced reactions are more complex, mainly because of two-and three-nucleon absorption processes.

Above the pion production threshold, the inelastic interactions are, again, handled by the resonance model.

Other pion-nucleon interactions proceed through the non-resonant channel and the p-wave channel with the formation of a Δ resonance. In nuclear matter, the Δ can either decay, resulting in elastic scattering or charge exchange, or interact with other nucleons, resulting in pion absorption. The width of the resonance is thus different from the free one. To account for this, the pion-nucleon total cross section used in PEANUT has been derived from the free one [21] in the following way: first, the resonant part has been extracted from the free cross section assuming for it a Breit-Wigner shape with an energy-dependent width [22]. After that, a "new" resonant cross section σ_r^A is calculated adding to the free width Γ_F the imaginary part of the (extra) width arising from nuclear medium effects. To this purpose the approach outlined in [23] has been adopted. The Δ effective width thus becomes:

$$\frac{1}{2}\Gamma_T = \frac{1}{2}\Gamma_F - Im\Sigma_\Delta \tag{4}$$

$\Sigma_\Delta = \Sigma_Q + \Sigma_2 + \Sigma_3$ as calculated by Oset et.al. [23]; Σ_Q, Σ_2 and Σ_3 are the partial widths for quasielastic scattering, two body and three body absorption (see ref. [23] for details). In addition, a two-body s-wave absorption cross section has been derived from the optical model [24]. Isospin relations have been extensively applied both to derive the pion-nucleon cross sections in any given charge configuration from the three experimentally known, and to weight the different interaction and decay channels of the Δ resonance [22, 25]. In s-wave absorption, the relative probability of absorption on a np pair or on a nn or pp pair, is assumed to be the same as in p-wave absorption. In the case of resonant reaction, the Δ is allowed to travel inside the nucleus according to its mean life before decaying.

Angular distributions of reaction products are sampled according to experimental data both for pion scattering (from free pion-nucleon) and pion absorption (from absorption on ^{3}He and deuterium).

2.6 Quantistic effects

The naive use of free hadron-nucleon cross sections would lead to hadron mean free paths in nuclei by far too short with respect to reality. Indeed there are many effects that influence the in-medium cross sections, and some of them are accounted for in FLUKA .

- Pauli blocking: Any secondary nucleon created in an intranuclear interaction must obey the Pauli exclusion principle, thus it must have enough energy to jump from the Fermi sea where it lies before the interaction to an unoccupied state, above the Fermi level.

- The formation zone [26] concept after pion or nucleon interactions. This concept has a strong analogy with the Landau-Pomeranchuk-Migdal [27] (LPM) effect which reduces electron bremsstrahlung and photon pair production at very high energies. Naively, it can be understood considering that hadrons are composite objects and that the typical time of strong interactions is of the order of 1 fm. If one thinks about the hadrons emerging from an inelastic interaction, it requires some time to them to "materialize" and be able to undergo further interactions. This time interval can be expressed as

$$t_{lab} \approx \frac{\hbar E_{lab}}{p_T^2 + M^2} \tag{5}$$

  This expression or, equivalently, the Stodolsky [26] one, is an approximation suitable for deep inelastic interactions, and is not fully covariant. As explained below, in case of elastic or quasi-elastic interactions a more rigorous approach can be followed

- Nucleon antisymmetrization effects [28], which decrease the probability for secondary particles to reinteract on a nucleon of the same type very close to the production point

- Nucleon-nucleon hard-core correlations which also prevent secondary particles to collide again too close to the production point. Typical hard-core radii used are in the range 0.5-1 fm

- "Coherence" length after (quasi)elastic or charge exchange scatterings. In analogy with the formation zone concept, such interactions cannot be localized better than the position uncertainty connected with the four-momentum transfer of the collision. Reinteractions occurring at distances shorter than the coherence length would undergo interference and cannot be treated anyway as independent interactions on other nucleons. The coherence length is the analogue of the formation time concept for elastic or quasielastic interactions. It has been applied to the secondaries in quasielastic neutrino-nucleon interactions, with the following recipe: given a two body interaction with four-momentum transfer $q = p_{1i} - p_{1f}$, (where in our case the subscript 1 refers to the *i*nitial or *f*inal lepton , and 2 to the hadron) the energy transfer seen in a frame where the particle 2 is originally at rest is given by

$$\Delta E_2 = \nu_2 = \frac{q \cdot p_{2i}}{m_2} \tag{6}$$

  From the uncertainty principle this ΔE corresponds to a indetermination in proper time given by $\Delta\tau \cdot \Delta E_2 = \hbar$, which boosted to the lab frames gives a coherence length

$$\Delta x_{lab} = \frac{p_{2lab}}{m_2} \cdot \Delta\tau = \frac{p_{2lab}}{m_2}\frac{\hbar}{\nu_2} \tag{7}$$

2.7 Preequilibrium emission

The INC step goes on until all nucleons are below 50 MeV and all particles but nucleons (typically pions) have been emitted or absorbed. To ensure continuity, however, secondary

nucleons with 10<E<50 MeV are transported by the INC algorithm till they either escape or reinteract in the nucleus. In the latter case no explicit interaction is performed: only an average Pauli rejection factor is applied and the exciton number is increased, leaving to the preequilibrium stage the further development of the configuration. At the end of the INC stage a few particles may have been emitted and the nuclear configuration is characterized by the total number of protons, Z^0_{pre}, and neutrons, N^0_{pre}, by the number of particle-like excitons (nucleons excited above the Fermi level), n_p ($n_p = n_{pro} + n_{neu}$), and of hole-like excitons (holes created in the Fermi sea by the INC interactions), n_h, by the "compound" nucleus excitation energy and by the "compound" nucleus momentum components, $p_{i\ comp}$. All the above quantities can be derived by proper counting what occurred during the INC stage and they represent the input configuration for the preequilibrium stage. The exciton formalism employed in PEANUT follows that of M. Blann and coworkers [29, 30, 31, 32], called Geometry Dependent Hybrid Model (GDH).

The preequilibrium process in the exciton model is described as a chain of steps, each step corresponding to a certain number of "excitons", where an exciton can be either a particle above the Fermi surface or a hole below the Fermi surface. The statistical assumption underlying the exciton model states that any partition of the excitation energy E among n, $n = n_h + n_p$, excitons has the same probability to occur. The nucleus proceeds in the chain through nucleon-nucleon collisions which increase the exciton number by two units, thus assuming that the probability of having an interaction that decreases the exciton number or lets it unchanged can be neglected (the so called "never come back" approximation). The chain stops, and equilibrium is reached, when either the exciton number n is sufficiently high ($n = \sqrt{2gE}$), where g is the single particle level density, or the excitation energy is below any emission threshold.

At each step there is a definite probability $P_{x,n}(\epsilon)$ of emitting a nucleon of type x and energy ϵ in the continuum. This probability can be factorized in two parts, one giving the fraction of n-exciton states in which one exciton is unbound and has energy ϵ in the continuum, the other giving the probability for the exciton to escape from the nucleus during its mean lifetime [29]:

$$P_{x,n}(\epsilon)\mathrm{d}\epsilon = \frac{\rho_{\mathrm{n}}(\mathrm{U},\epsilon)\mathrm{g}\mathrm{d}\epsilon}{\rho_{\mathrm{n}}(\mathrm{E})}\frac{\mathrm{r_c}(\epsilon)}{\mathrm{r_c}(\epsilon)+\mathrm{r_+}(\epsilon)} \tag{8}$$

where U is the residual nucleus excitation energy ($U = E - \epsilon - B_{en}$), and $\rho_n(E)$ is the density (MeV^{-1}) of exciton states, and is given by:

$$\rho_n(E) = \frac{g(gE)^{n-1}}{n!(n-1)!} \tag{9}$$

$r_c(\epsilon)$ is the rate of emission in the continuum, and is related to the cross section of the inverse process (σ_{inv}) by the detailed balance principle:

$$r_c = \sigma_{inv}\frac{\epsilon}{g_x}\frac{(2s+1)\,8\pi m}{h^3} \tag{10}$$

and $r_+(\epsilon)$ is the exciton reinteraction rate. The $r_+(\epsilon)$ can be calculated from the nucleon mean free path in nucleear matter [33] or from the optical model.

This formulation has been refined in the GDH [30] to account for the experimentally established importance of peripheral collisions. All position dependent parameters (density, Fermi energy, etc) are no longer constant, but depend on the impact parameter, and

the exciton state density is modified by the assumption that any hole-like exciton cannot carry an excitation energy larger than the local Fermi energy.

In the PEANUT implementation of GDH tere are a few modifications, regarding mainly the way the nuclear geometry is accounted for, inverse cross sections, and exciton reinteraction rates.

Moreover, a non-isotropic angular distribution has been implemented in PEANUT , following the fast particle approximation[43, 44]. In this model the angular orientation of the nucleus at each step is defined by the direction of the fast particle, which changes gradually in a series of two-body collisions. The transition rate between different exciton states is supposed to be factorizable in an energy-dependent and an angle-dependent factor.

2.8 Benchmarks

Many benchmarks showing good agreement between PEANUT results and nuclear reaction data can be found in the literature [1, 2, 3, 4, 5]. We report here a couple of examples for completeness.

The only warning to be issued about the reliability of PEANUT results when used for neutrino interactions is that most benchmarks are relative to hadron-nucleus interactions, thus are more sensitive to the skin of the nuclear density due to the short mean free path of hadrons in nuclei. Neutrinos, conversely, explore the whole nucleus, with an interaction probability that is proportional to the local nuclear density. There are indeed a few processes which feel the nuclear core in a way similar to neutrino interactions, i.e. photon induced reactions. Unfortunately few experimental data are available for photonuclear interactions in the energy range of interest for neutrino interactions. Other processes, even though not volume dependent like neutrino interactions, are anyway preferentially sensitive to high density zones of nuclei. Two and three nucleon pion absorption is one of these processes, since naively, absorption probabilities scale like ρ^2 and ρ^3 respectively. This warning does not mean that neutrino interactions were described in terms of mean free paths and geometrical locations of neutrino-nucleon interactions similar to those of hadron-nucleus interactions. Indeed, as explained in the following paragraph, the correct distribution of neutrino interactions has been adopted.

3 Nuclear effects in neutrino-nucleus interactions

As a first step, 10000 events for ν_τ, ν_μ and ν_e quasielastic interactions on free nucleons have been generated with the WBB beam spectrum [6] (the ν_τ spectrum is taken equal to the ν_μ spectrum, while the ν_e spectrum is the expected spectrum for the ν_e contamination in the ν_μ beam). In the ν_τ events, τ are decayed to leptons.

Final state particles are inserted into Argon nuclei and assumed as initial configuration for PEANUT. Due to the Fermi motion of the target nucleons, a recorrection of the kinematics is necessary. In doing this, the center of mass energy of the free system is preserved,

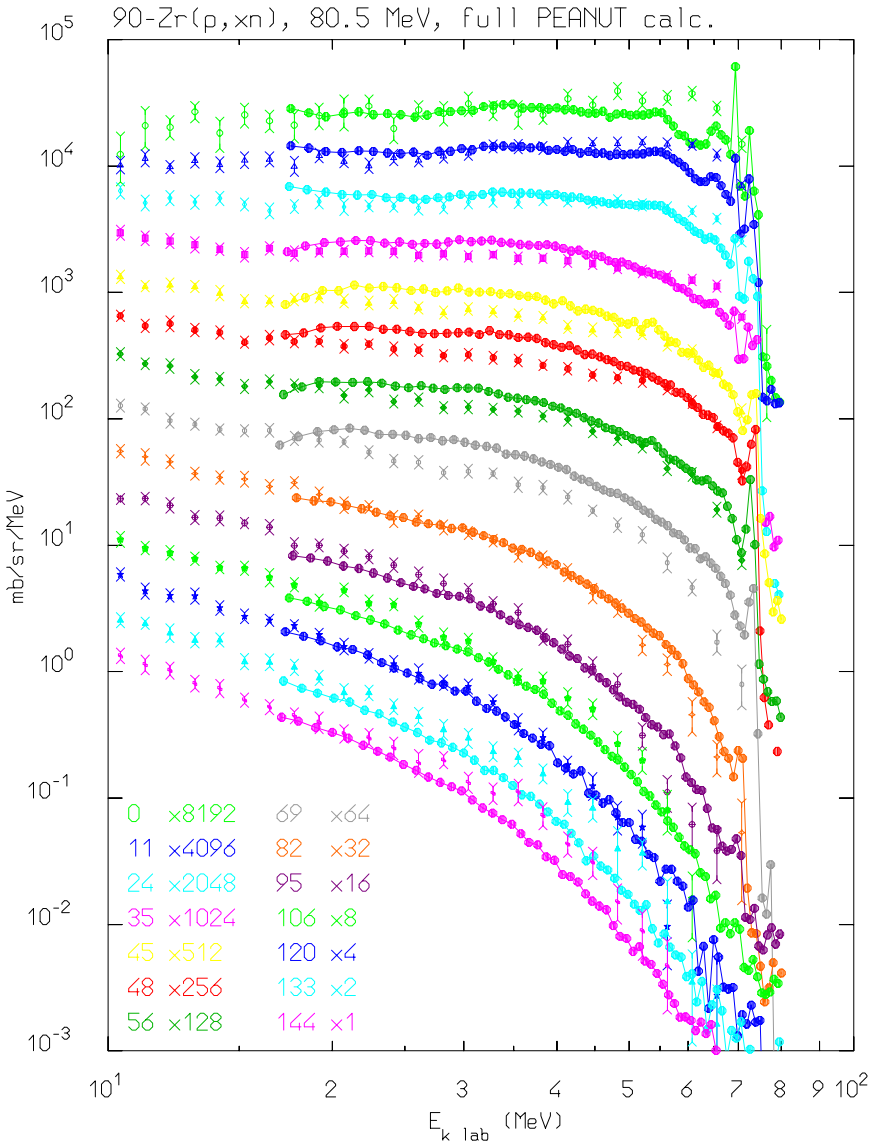

Figure 1: Double differential distribution of neutrons from ^{90}Zr(p,xn) at 80.5 MeV. Dots connected by a line: exp. data from [34, 35]. Symbols with errors : PEANUT

and the incident neutrino direction is fixed; as a consequence, all the particle momenta are scaled and rotated. In more detail, the implementation is performed according to the following procedure:

- The target nucleon (a neutron for quasielastic events) is randomly selected among all available ones. In practice the position $\vec{r}$ of the hitten neutron is selected according to:

$$P(\vec{r})\mathrm{d}^3\vec{\mathrm{r}} = \frac{\rho_{\mathrm{n}}(\mathrm{r})\mathrm{d}^3\vec{\mathrm{r}}}{\mathrm{N}} \tag{11}$$

- The Fermi momentum, $\vec{p}_f$ and hence the Fermi energy, E_{kf}, of the target nucleon is

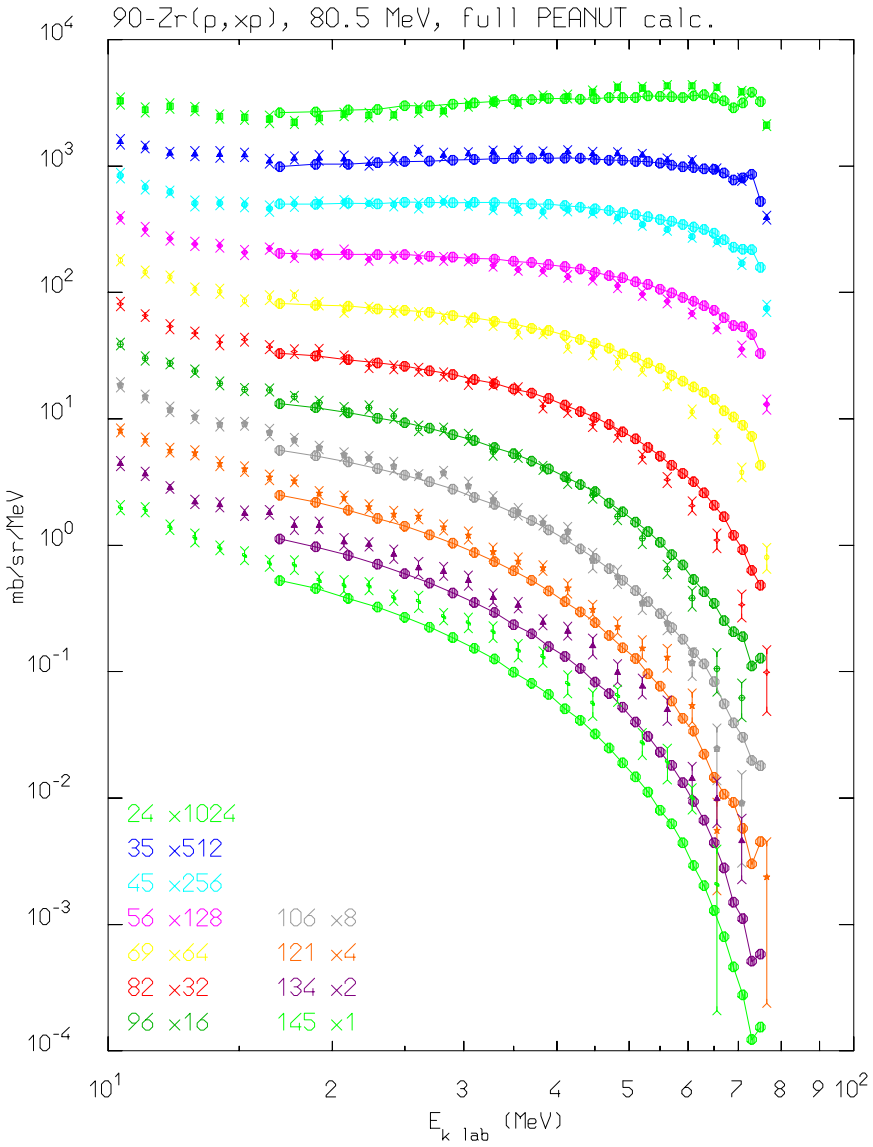

Figure 2: As in fig. 1 for emitted protons

selected according to the standard distribution and the local nuclear density

- A ν-neutron interaction is randomly selected among those generated and recorded on file. Let $p_{\nu 0}$ be the neutrino energy in the frame where the target nucleon is at rest and $\sqrt{s}$ the centre-of-mass energy of the ν-nucleon interaction.

- Assuming the neutrino incident along direction $\vec{u}$, the neutrino energy in the system where the nucleus is at rest, p_ν, can be obtained from:

$$s = m(m + 2p_{\nu 0}m) = (p_\nu + E_{kf} + m)^2 - (\vec{p}_f + p_\nu \vec{u})^2 \quad (12)$$

$$p_\nu = \frac{mp_{\nu 0}}{m + E_{kf} - \vec{p}_f \cdot \vec{u}} \quad (13)$$

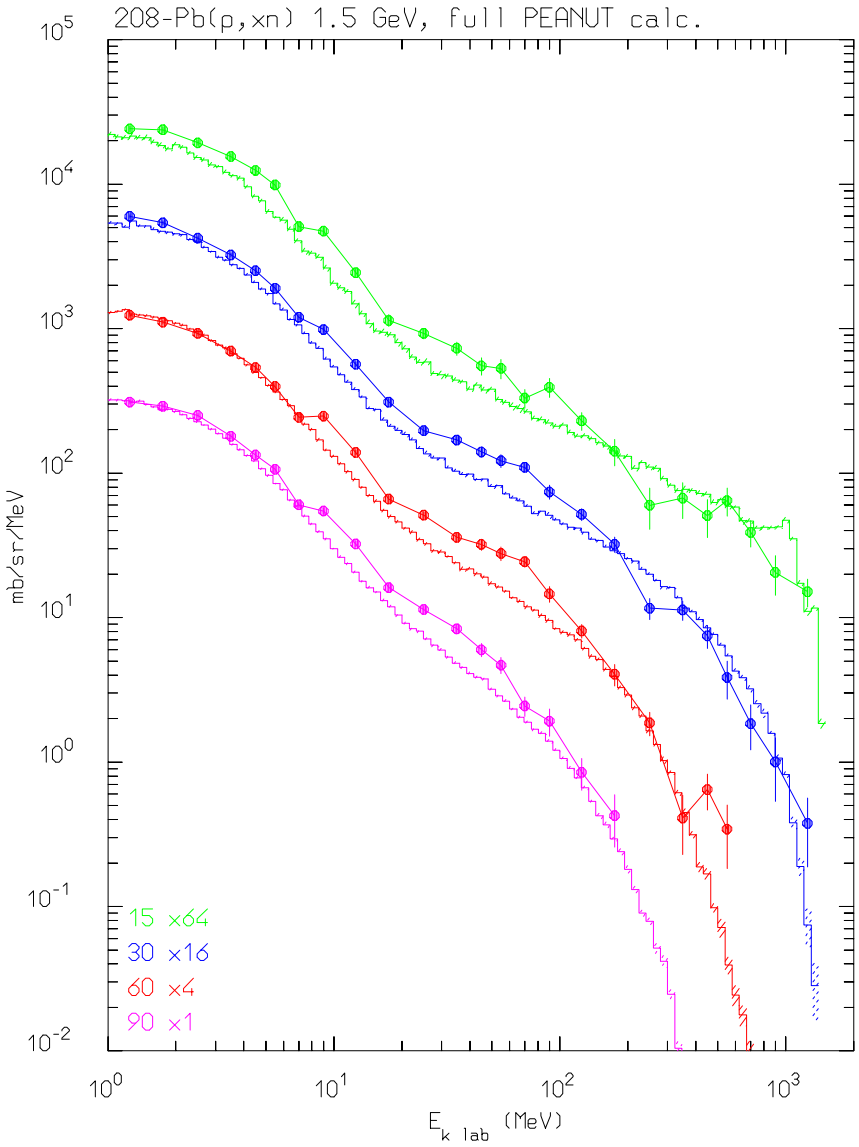

Figure 3: Neutron double differential distribution from ^{208}Pb(p,xn) at 1.5 GeV. Dots: expt. data from [36]. Histogram : PEANUT

In general p_ν is somewhat different from $p_{\nu 0}$. Therefore a slight distorsion of interacting neutrino spectra (originally chosen according to $\Phi(p_{\nu 0}) \cdot \sigma_{qe}(p_{\nu 0})$) does result from this procedure. Such a distorsion cannot be avoided and does not have any major impact. In the future, an on line coupling of the neutrino-nucleon event generator and PEANUT will allow to overcome completely this problem.

- The interaction is "performed" in the frame where the target nucleon is at rest, through a suitable Lorentz boost:

$$\vec{p}_{\nu 0} \quad = \quad \vec{p}_\nu - \vec{\eta}(p_{\nu 0} - \frac{\vec{\eta} \cdot \vec{p}_\nu}{\gamma + 1}) \tag{14}$$

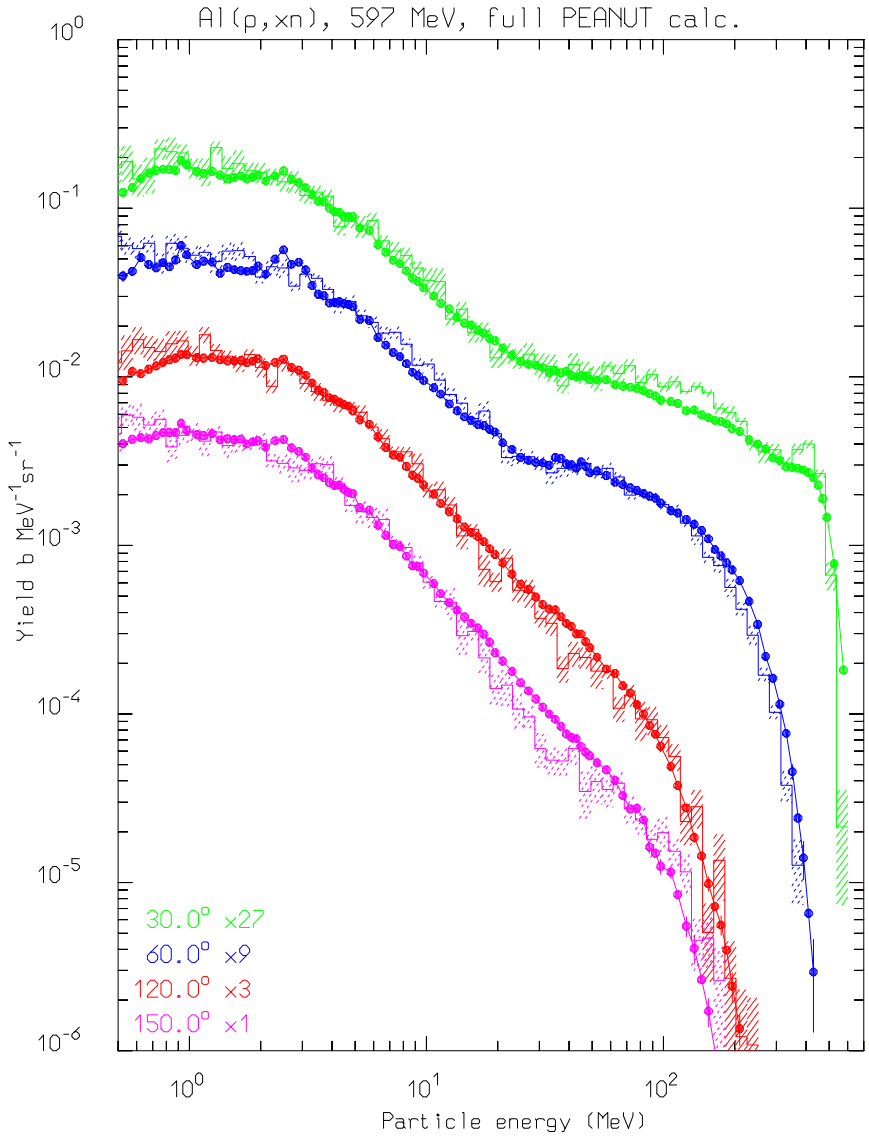

Figure 4: Neutron double differential distribution from Al(p,xn) at 0.597 GeV. Dots: exp. data from [37]. Histogram : PEANUT

$$\vec{\eta} = \frac{\vec{p}_\nu + \vec{p}_f}{\sqrt{s}} \tag{15}$$

$$\gamma = \frac{p_\nu + E_{kf} + m}{\sqrt{s}} \tag{16}$$

In general $\vec{p}_{\nu 0}$ is not parallel to $\vec{p}_\nu$.

Also 10000 events for ν_τ, ν_μ and ν_e interactions on free nucleons with Δ production have been generated (Gli spettri di nu(RES) hanno i seguenti valori medi: nue=56, numu=41, nutau=28 per i QE i valori sono nue=37, numu=25, nutau=26 cioe' nutau=numu ??); in the events sample $\Delta^{++} \to p\pi^+$, $\Delta^+ \to p\pi^0$and $\Delta^+ \to n\pi^+$are present. In the ν_τ events,

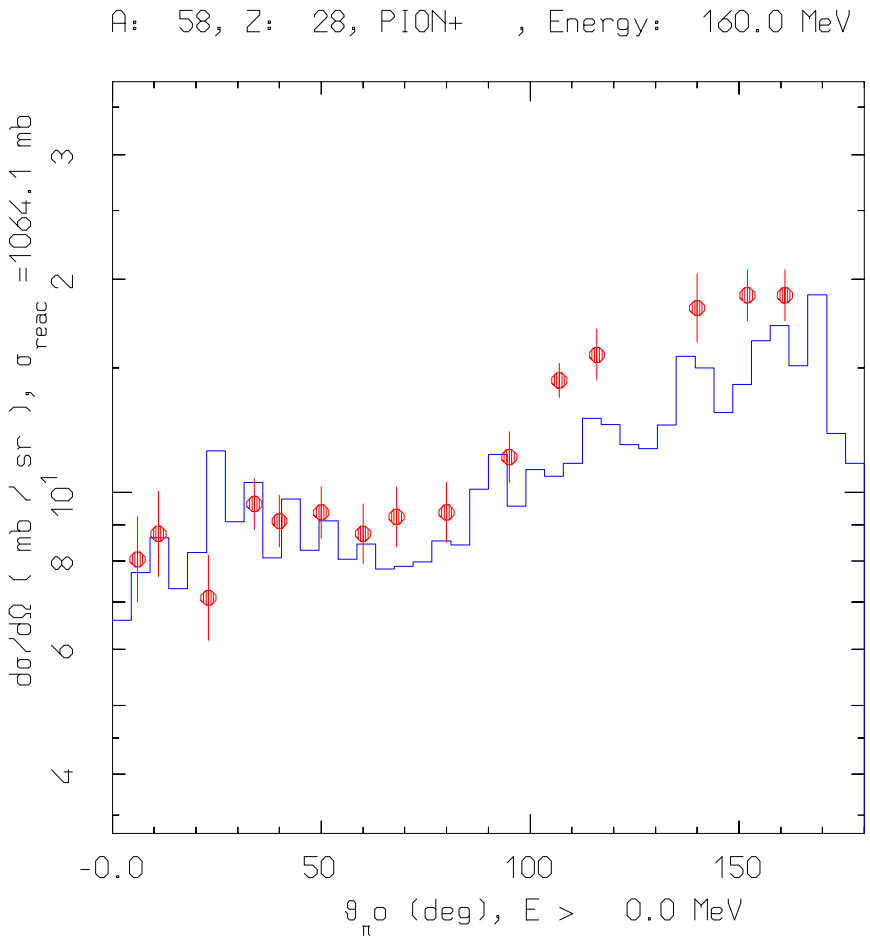

Figure 5: Angular distribution of positive pions following ^{58}Ni(π^+,π^+x). Dots:exp. data from [38, 39]. Histogram: PEANUT

τ are always decayed to electrons. The events with Δ resonances production have been treated in a similar way as the quasielastic events.

3.1 Effects on final states kinematics

The kinematics of the final states of the free nucleons and bound nucleons QE neutrino interactions have been compared. The free nucleon interactions of the three neutrino species give a lepton and a proton ($< p_p > \sim$ 800 MeV) in the final state, while the bound nucleons interactions have in the final state a lepton, one (or more) residual nucleus ($< p_{res\ nucleus} > \sim$ 250 MeV) and some protons, neutrons, γ-rays and charged and neutral pions with the average multiplicities and momenta given in Table 1 (values are very similar

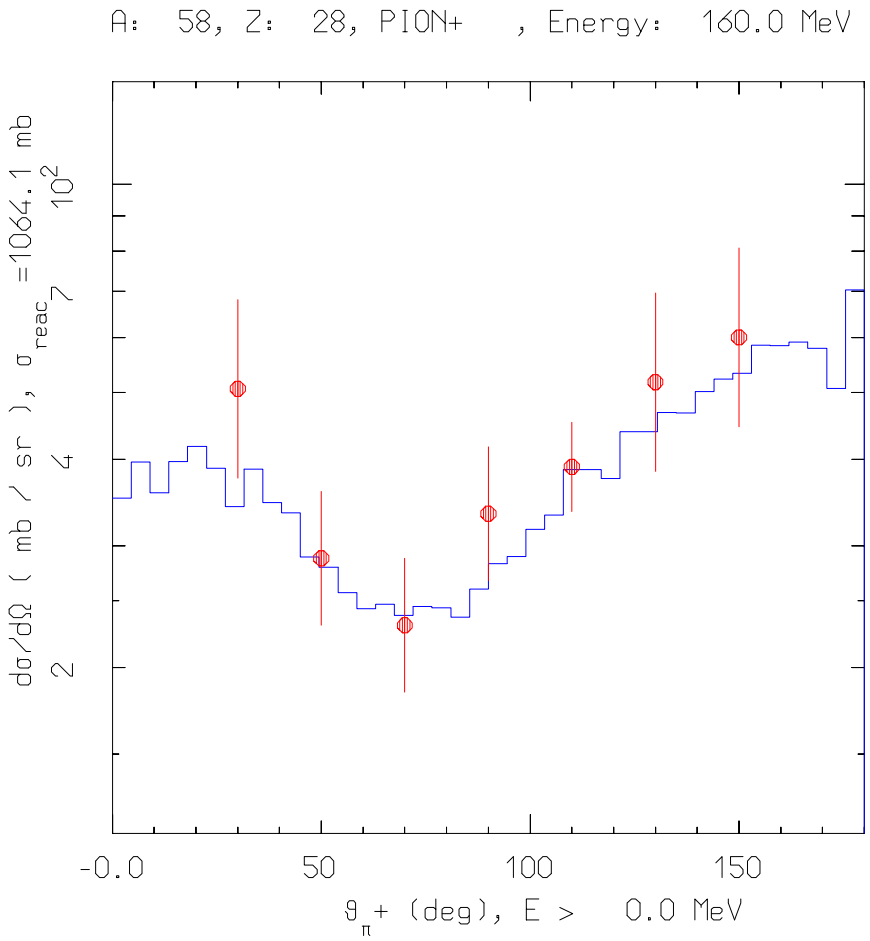

Figure 6: Angular distribution of neutral pions following ^{58}Ni(π^+,π^0x). Dots: exp. data from [38, 39]. Histogram: PEANUT

for ν_e, ν_μ, ν_τ).

In Fig. 9(a) the momentum spectra of final proton in QE ν_e-free nucleon interactions and all final protons in QE ν_e-bound nucleon interactions are compared; in Fig. 9(b) the momentum spectra of the leading final proton in the two interaction types are compared. In Fig. 10(a) the angular spectra of final proton in QE ν_e-free nucleon interactions and all final protons in QE ν_e-bound nucleon interactions are compared; in Fig. 10(b) the angular spectra of the leading final proton in the two interaction types are compared.

The kinematics of the final states of the free nucleons and bound nucleons Δ^+ and Δ^{++} production neutrino interactions have also been compared. The free nucleon interactions of the three neutrino species with Δ resonances production give a lepton, a charged or neutral pion ($< p_\pi > \sim$ 400-600 MeV) and a nucleon (proton or a neutron) ($< p_{nucleon} > \sim$ 800-1000 MeV) in the final state, while the bound nucleons interactions have in the final

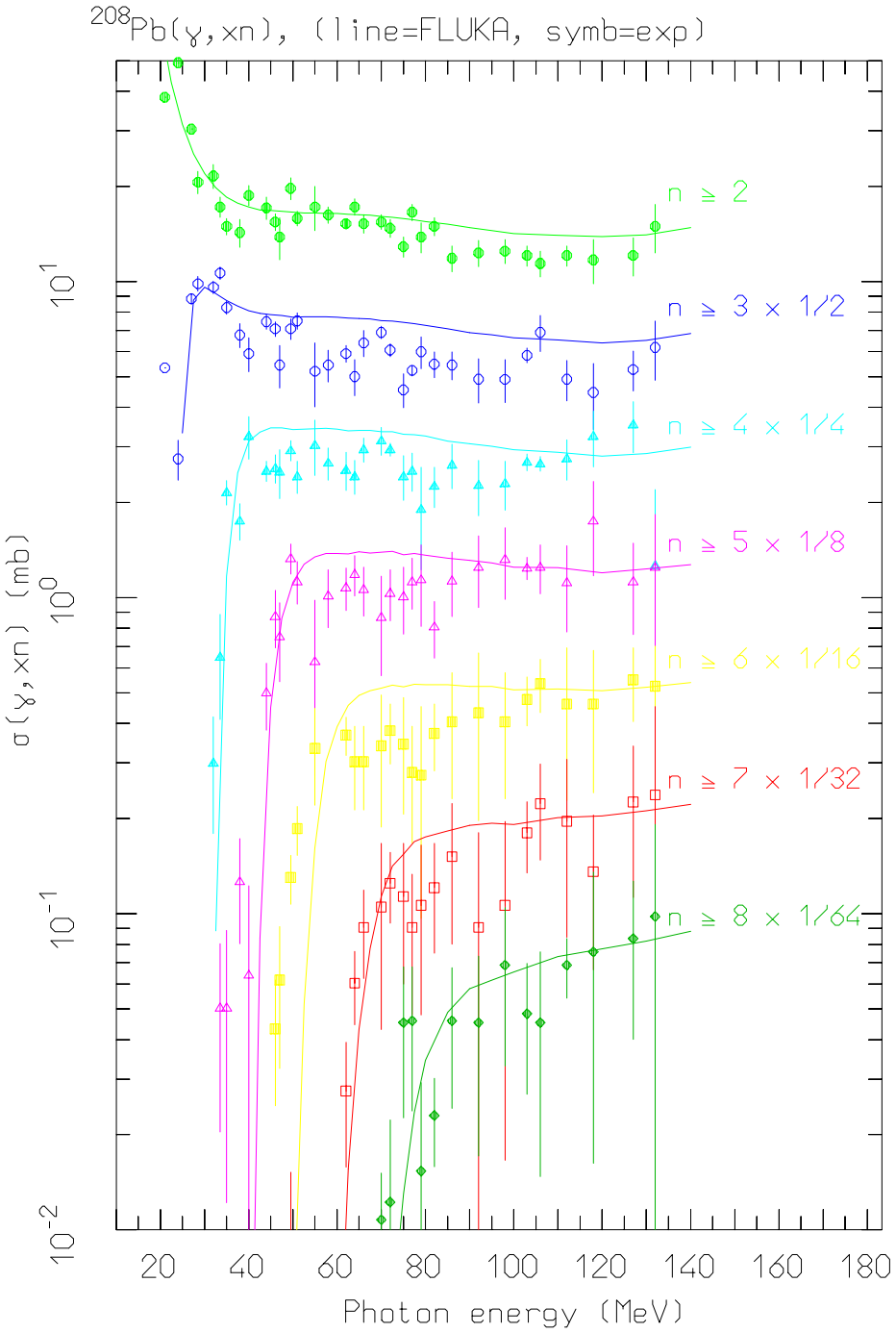

Figure 7: Excitation functions of ^{208}Pb(γ,xn) reactions for different neutron multiplicities. Symbols: exp. data from [40]. Lines: PEANUT

state a lepton, one (or more) residual nucleus ($< p_{res\ nucleus} > \sim$ 300 MeV) and charged and neutral pions and some protons, neutrons, γ-rays with the average multiplicities and momenta given in Table 2 (values are also here very similar for ν_e, ν_μ, ν_τ).

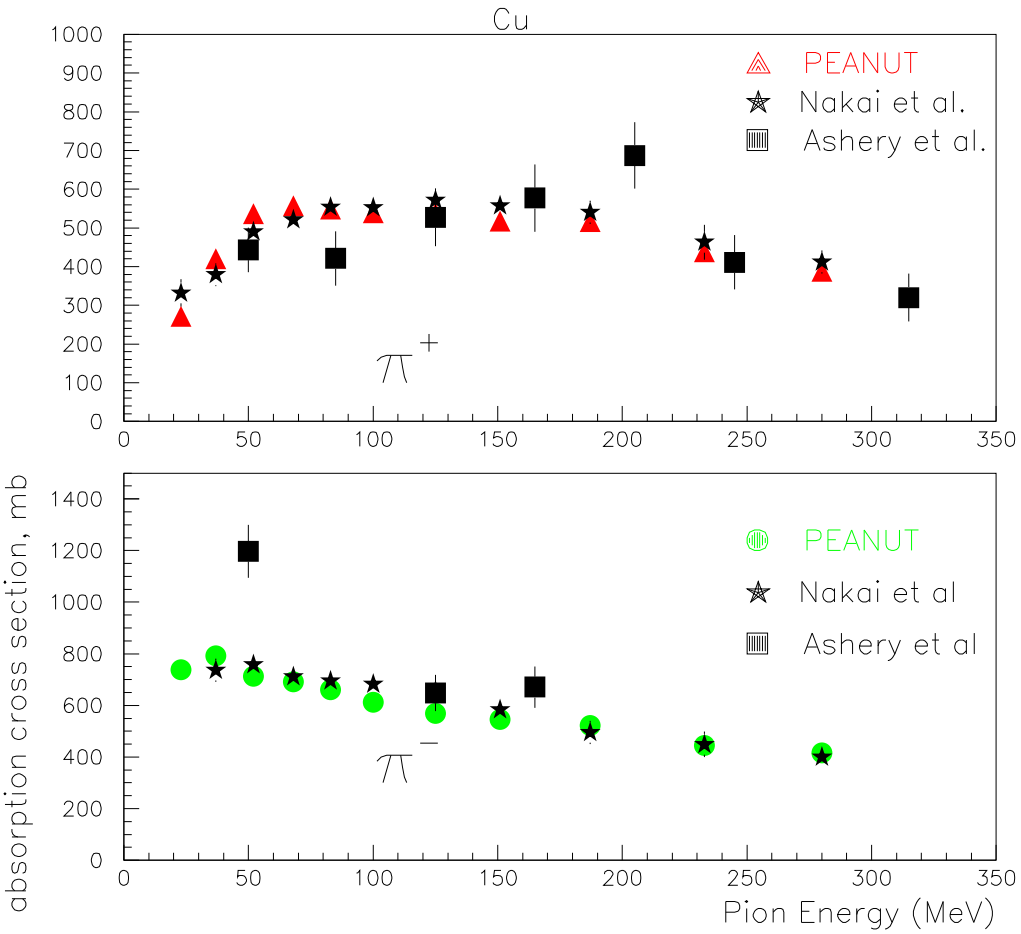

Figure 8: Pion absorption cross section in Cu as a function of lab pion energy; Data are from [41, 42]

Table 1: *Final state in bound nucleon QE interactions*

final particles	< *multiplicity* >	< *momentum* > GeV / c
protons	1.46	0.47
neutrons	1.3	0.16
charged pions	0.025	0.35
pizero's	0.015	0.36
γ-rays	2.36	0.0025

Table 2: *Final state in bound nucleon interactions with* Δ *production*

final particles	$\Delta^{++} \to p\pi^+$ $< multipl. >$	$< p >$ GeV	$\Delta^{+} \to p\pi^0$ $< multipl. >$	$< p >$ GeV	$\Delta^{+} \to n\pi^+$ $< multipl. >$	$< p >$ GeV
protons	2.58	0.42	2.47	0.45	1.75	0.28
neutrons	2.94	0.16	2.47	0.20	2.98	0.38
charged pions	0.61	0.44	0.09	0.30	0.76	0.59
pizero's	0.05	0.26	0.66	0.59	0.05	0.30
γ-rays	2.19	0.0021	2.31	0.0026	2.37	0.0025

In Fig. 12(a) the momentum spectra of final pion in ν_e-free nucleon interactions and the final pion in ν_e-bound nucleon interactions are compared for Δ^{++} events; in Fig. 12(b) the momentum spectra of all final protons in the two interaction types are compared . In Fig. 13(a) the momentum spectra of final pion in ν_e-free nucleon interactions and the final pion in ν_e-bound nucleon interactions are compared for $\Delta^{+} \to p\pi^0$events; in Fig. 13(b) the momentum spectra of all final protons in the two interaction types are compared . In Fig. 14(a) the momentum spectra of final pion in ν_e-free nucleon interactions and the final pion in ν_e-bound nucleon interactions are compared for $\Delta^{+} \to n\pi^+$; in Fig. 14(b) the momentum spectra of all final neutrons in the two interaction types are compared . The plots in the above figures are always done for the events with 1 pion in the final state.

3.2 Effects on acceptances for QE events and missing momentum

As we have seen the final state of QE ν events on free and bound nucleons are different, so we expect that experimental acceptances will be different if nuclear effects are or not taken into account.

If we define a "QE ν event in Icarus" as an event satisfying the following criteria: presence of a lepton and one proton with T_p >150 MeV (with no pions with T_π >15 MeV), we find that the acceptance of these criteria applied to free and bound nucleon interactions for the three neutrino species are very similar and goes from $\sim$ 60% for free nucleon interactions to $\sim$ 42% for bound nucleon interactions.

The most important nuclear effect is an apparent missing momentum in the interaction, due to the unseen energy, taken away by the residual nucleus, by neutrons and by undetected low energy particles (γ, p, π). For that reason , while in the free nucleon ν_e and ν_μ interactions the missing momentum is zero, in the bound nucleon interactions the missing momentum is different from zero.

The situation is of course different in the case of ν_τ beam where a real missing momentum is present ($< p_{miss} > \sim$ 700 MeV) also in free nucleon interactions, due to the two neutrinos from the $\tau \to$ e decay. In this case the missing momentum distribution is not so much modified by nuclear effects.

Calculating the visible momentum in the event summing up the lepton, all protons with $T_p > 60$ MeV, all pions with $T_\pi > 15$ MeV we obtain the plots of Fig. 11, where the distribution of missing momentum for ν_e QE events on bound nucleon is compared to the distributions of missing momentum for ν_τ QE events on free and bound nucleons.

If a criterium to recognize ν_τ events from ν_e interactions would be to have a missing momentum > 400 MeV, the acceptance would be $\sim 4.\%$ for ν_e and ν_μ and $\sim 33\%$ for ν_τ. So there will be a contamination of ν_e events in the selected ν_τ events sample: this contamination can be reduced using other cuts for example on lepton momentum and direction.

3.3 Effects on acceptances for Δ events and missing momentum

As we have seen the final state of Δ ν events on free and bound nucleons are different, so we expect that experimental acceptances will be different if nuclear effects are or not taken into account.

If we define a "$\Delta^{++} \rightarrow p\pi^+\nu$ event in Icarus", a" $\Delta^+ \rightarrow p\pi^0$event in Icarus" and a "$\Delta^+ \rightarrow n\pi^+$event in Icarus as an event satisfying respectively the following criteria: presence of a lepton and one charged pion with T_π >15 MeV and a proton with T_p >60 MeV, a lepton and one neutral pion with T_π >15 MeV and a proton with T_p >60 MeV and a lepton and one charged pion with T_π >15 MeV and no protons with T_p >60 MeV, we find that the acceptance of these criteria applied to free and bound nucleons interactions for the three neutrino species are very similar. The acceptance is $\sim 95\%$, $\sim 95\%$ and $\sim 100\%$ respectively for the three resonances produced in free nucleon interactions, due to the request on the proton energy; the acceptance is lower for bound nucleons interactions, where a ν event with Δ production can be classified as a QE event (according to the criteria described in previous section: a lepton and one proton with T_p >150 MeV) or as an event with more than one fast proton (T_p >150 MeV) or as an event with a pion with a different charge or with more than 1 pion or as an event with only very slow protons ($T_p < 60MeV$) accompanied by neutrons and γ-rays, as it can be seen from the values reported in Table 3 for the ν_e interactions.

As it can be from Table 3 a not negligible percentage of Δ^+ and Δ^{++} events are classified as QE events.

The most important nuclear effect is again an apparent missing momentum in the ν_e and ν_μ interactions where there is no real missing momentum ($\Delta^{++} \rightarrow p\pi^+$and $\Delta^+ \rightarrow p\pi^0$), due to the unseen energy, taken away by the residual nucleus, by neutrons and by undetected low energy particles (γ, p, π). In the $\Delta^+ \rightarrow n\pi^+$events there is a real missing momentum due to the neutrons, that are detected with difficulty.

The situation is of course different in the case of ν_τ beam where a real missing momentum is present ($< p_{miss} >\sim 700$ MeV) also in free nucleon $\Delta^{++} \rightarrow p\pi^+$and $\Delta^+ \rightarrow p\pi^0$interactions, due to the two neutrinos from the $\tau \rightarrow$ e decay. In this case the missing momentum distribution is not so much modified by nuclear effects.

Calculating the visible momentum in the event summing up the lepton, all protons with $T_p > 60$ MeV, all pions with $T_\pi > 15$ MeV we obtain the plots of Fig. 15 and 16 where

Table 3: *Acceptances of bound nucleon interactions with Δ production*

classification	$\Delta^{++} \to p\pi^+$	$\Delta^+ \to p\pi^0$	$\Delta^+ \to n\pi^+$
"QE event"	19%	15%	10%
1 charged pion event	57%	5%	69%
1 neutral pion event	3%	62%	3%
"$\Delta^{++} \to p\pi^+$"	42%	3%	10%
"$\Delta^+ \to p\pi^0$"	2%	48%	1%
"$\Delta^+ \to n\pi^+$"	11%	0	56%
more than 1 pion	3 %	4%	5 %
no pions, $>$ 1p with $T_p > 150$MeV	7%	5%	2%
no pions, and protons with $T_p > 60$MeV	9%	7%	9%
no pions, no protons with $T_p > 60$MeV	2%	2%	3%

the distribution of missing momentum for ν_e $\Delta^{++} \to p\pi^+$and $\Delta^+ \to p\pi^0$events on bound nucleon are compared to the distributions of missing momentum for ν_τ Δ production events on free and bound nucleons.

If a criterium to recognize a $\Delta^{++} \to p\pi^+$or a $\Delta^+ \to p\pi^0\nu_\tau$ events from the equivalent ν_e interactions would be to have a missing momentum $>$ 400 MeV, the acceptance would be 11(5)% for ν_e $\Delta^{++} \to p\pi^+$and 46(35)% for ν_τ $\Delta^{++} \to p\pi^+$and 10(4)% for ν_e $\Delta^+ \to p\pi^0$and 53(43)% for ν_τ $\Delta^+ \to p\pi^0$, simply asking for 1 charged or neutral pion (or also asking for a proton with $T_p > 60$ MeV).

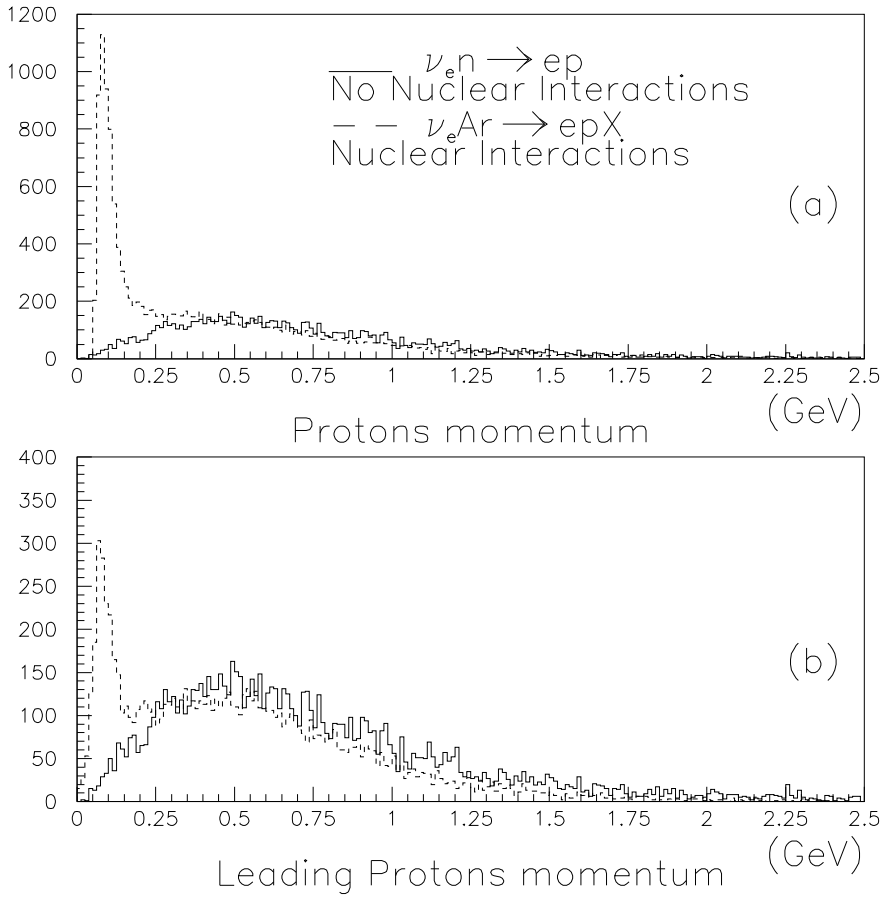

Figure 9: *Momentum of final protons in QE ν interactions (plot (a)); momentum of leading final proton in ν interactions (plot (b))*

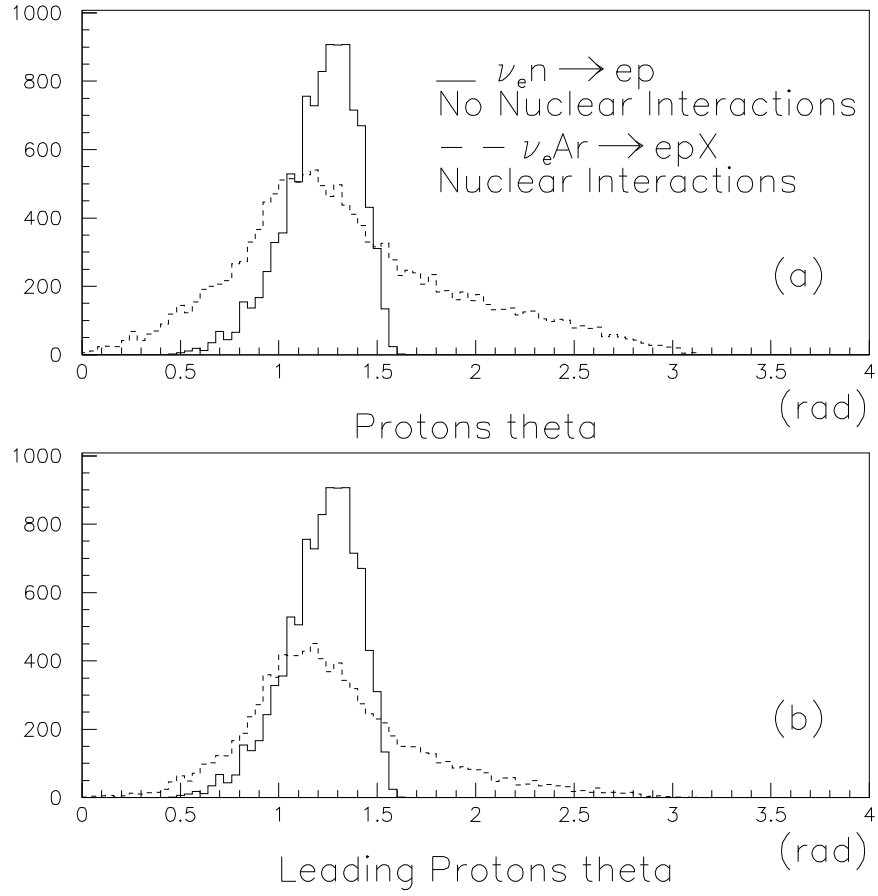

Figure 10: *Angular distribution of final protons in QE ν interactions (plot (a)); angular distribution of leading final proton in ν interactions (plot (b))*

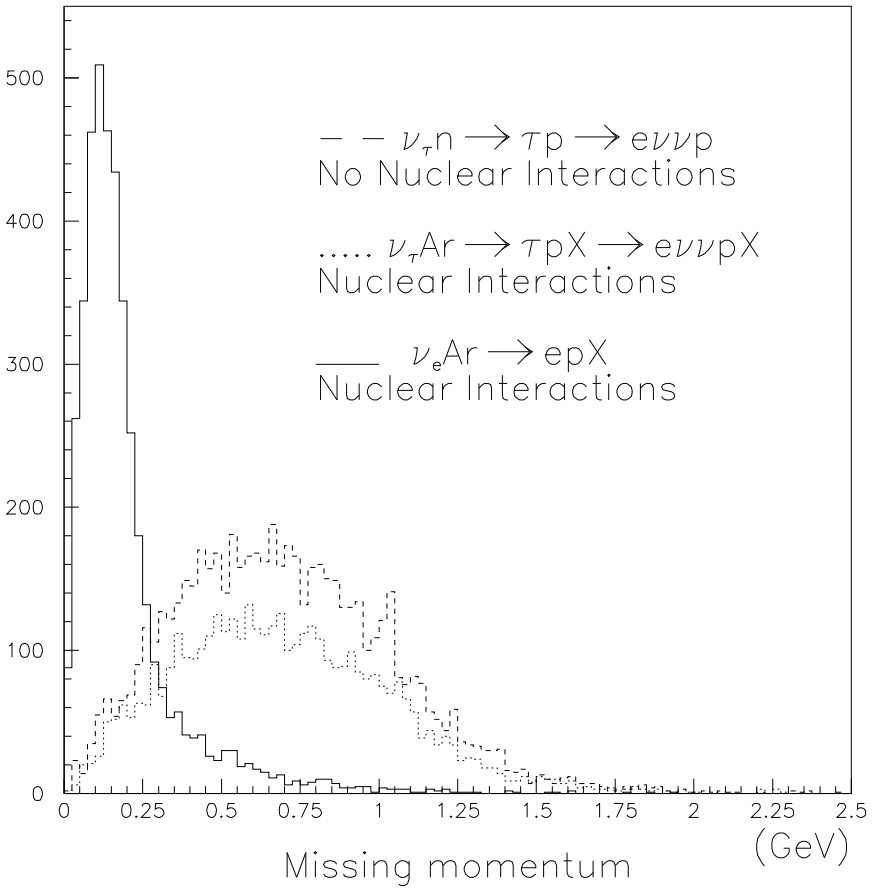

Figure 11: *Missing momentum in QE ν_e bound nucleon interactions (full line); in QE ν_τ free nucleon interactions (dashed line); in QE ν_τ bound nucleon interactions (dotted line)*

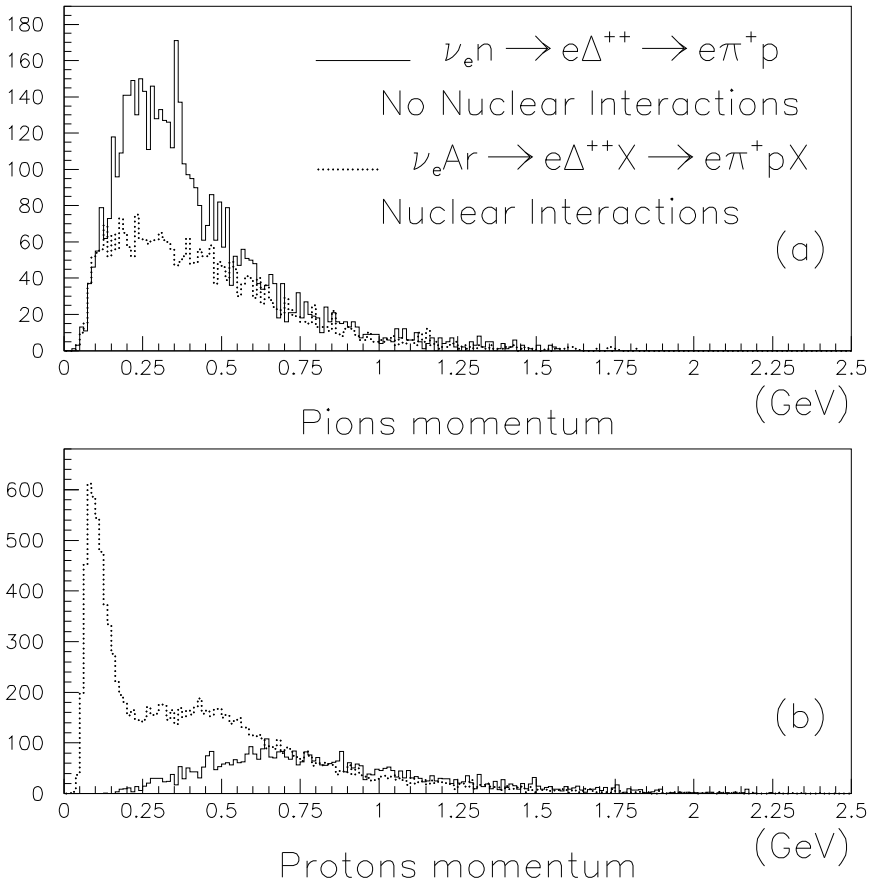

Figure 12: *Momentum of final charged pion in ν interactions with Δ^{++} production (plot (a)); momentum of final protons in ν interactions with Δ^{++} production (plot (b))*

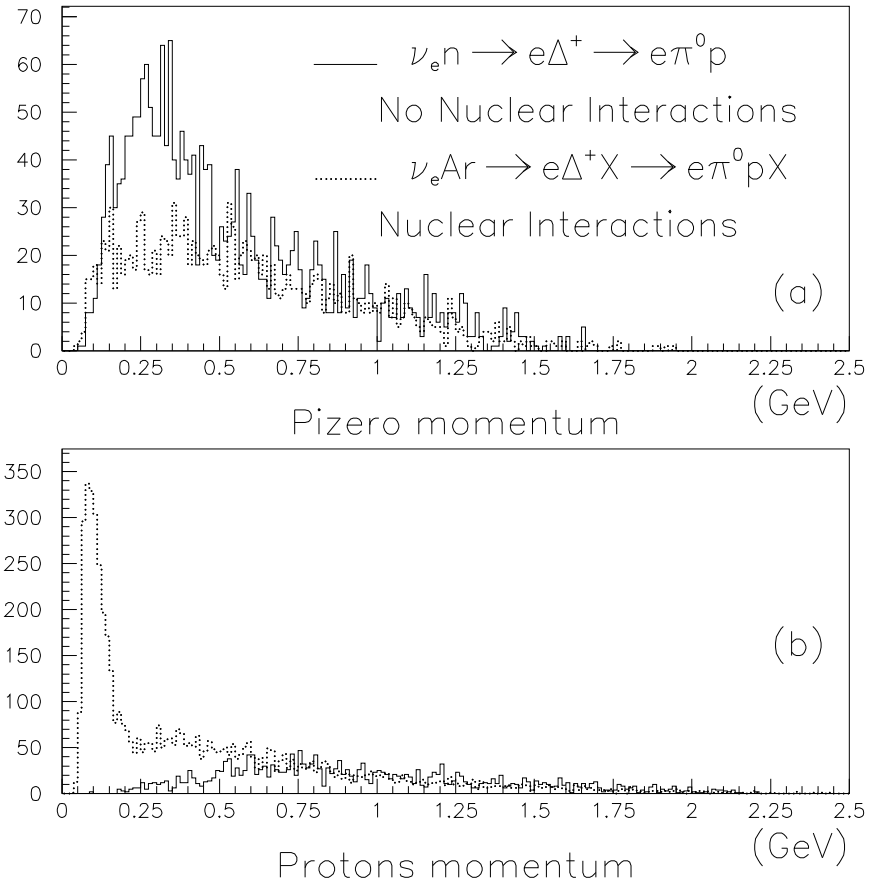

Figure 13: *Momentum of final charged pion in ν interactions with $\Delta^+ \rightarrow p\pi^0$production (plot (a)); momentum of final protons in ν interactions with $\Delta^+ \rightarrow p\pi^0$production (plot (b))*

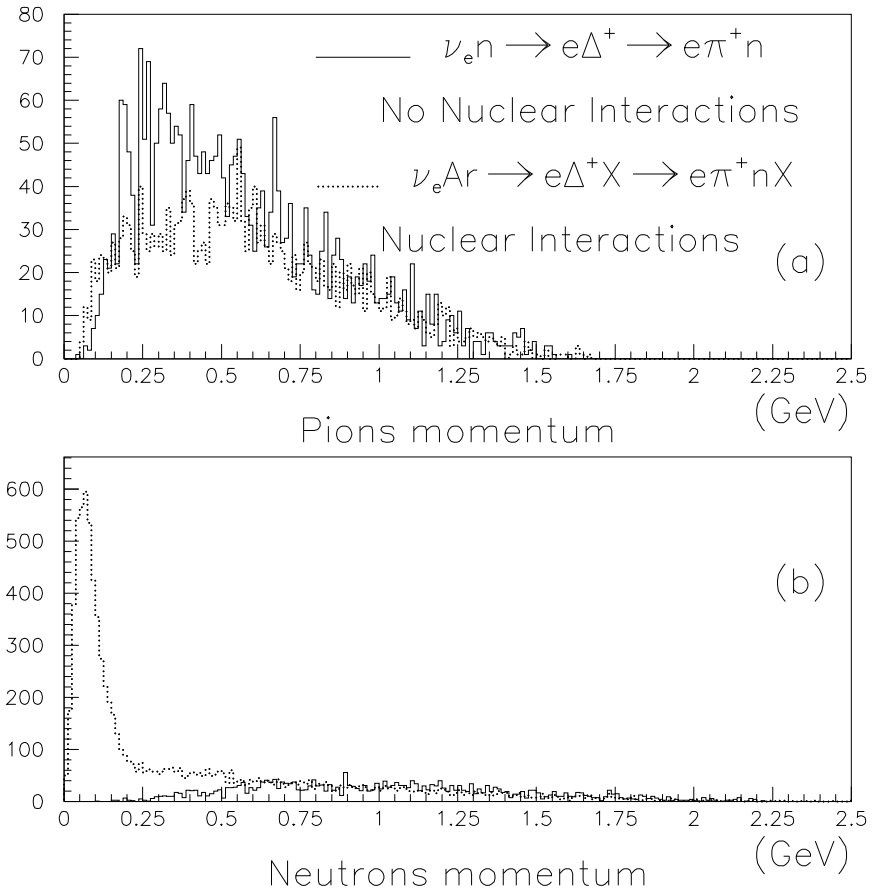

Figure 14: *Momentum of final charged pion in ν interactions with $\Delta^+ \rightarrow n\pi^+$production (plot (a)); momentum of final protons in ν interactions with $\Delta^+ \rightarrow n\pi^+$production (plot (b))*

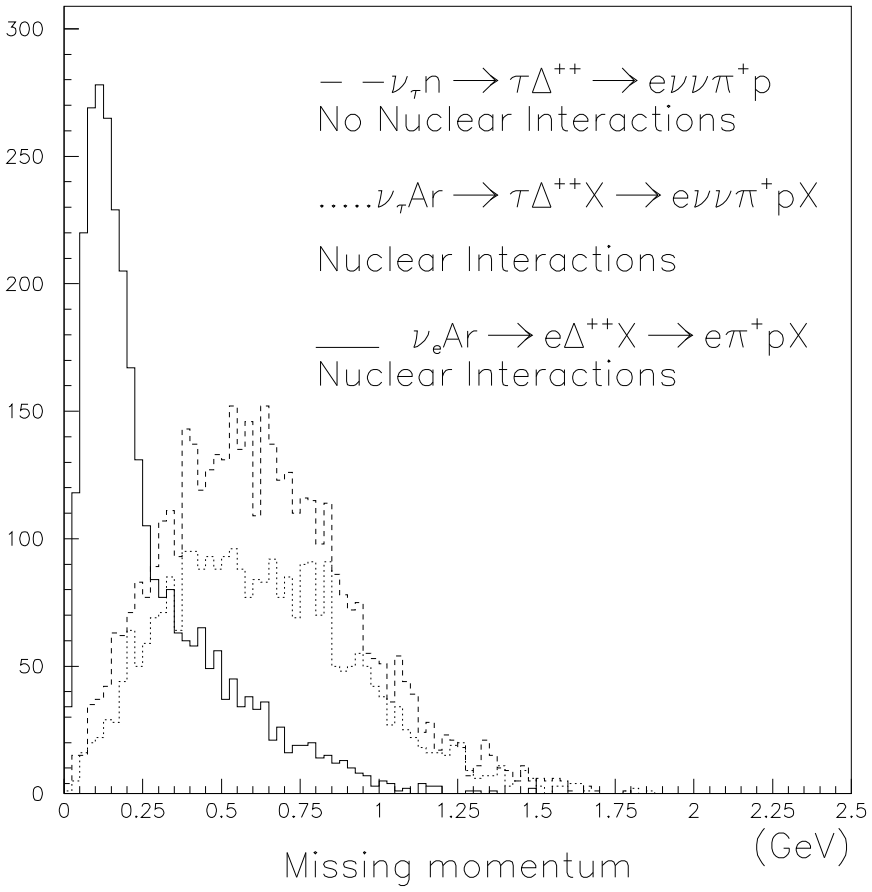

Figure 15: *Missing momentum in ν_e bound nucleon $\Delta^{++} \rightarrow p\pi^+$ interactions (full line); in ν_τ free nucleon interactions (dashed line); in ν_τ bound nucleon interactions (dotted line)*

References

[1] A. Fassò, A. Ferrari, J. Ranft, P. R. Sala, G. R. Stevenson, and J. M. Zazula, Proc. of the workshop on *Simulating Accelerator Radiation Environment, SARE*, Santa Fè, 11-15 january (1993), (A. Palounek ed., Los Alamos LA-12835-C 1994), p. 134.

[2] A. Fassò, A. Ferrari, J. Ranft and P. R. Sala, Proc. of the *IV International Conference on Calorimetry in High Energy Physics*, La Biodola (Elba), September 19-25 1993, (A. Menzione and A. Scribano eds., World Scientific 1994), p. 493.

[3] A. Ferrari, and P. R. Sala, Proc. of the *MC93 Int. Conf. on Monte-Carlo Simulation in High-Energy and Nuclear Physics*, Tallahassee, Florida, 22-26 february (1993), (World Scientific ed. 1994), p. 277; A. Fassò, A. Ferrari, J. Ranft, and P. R. Sala,

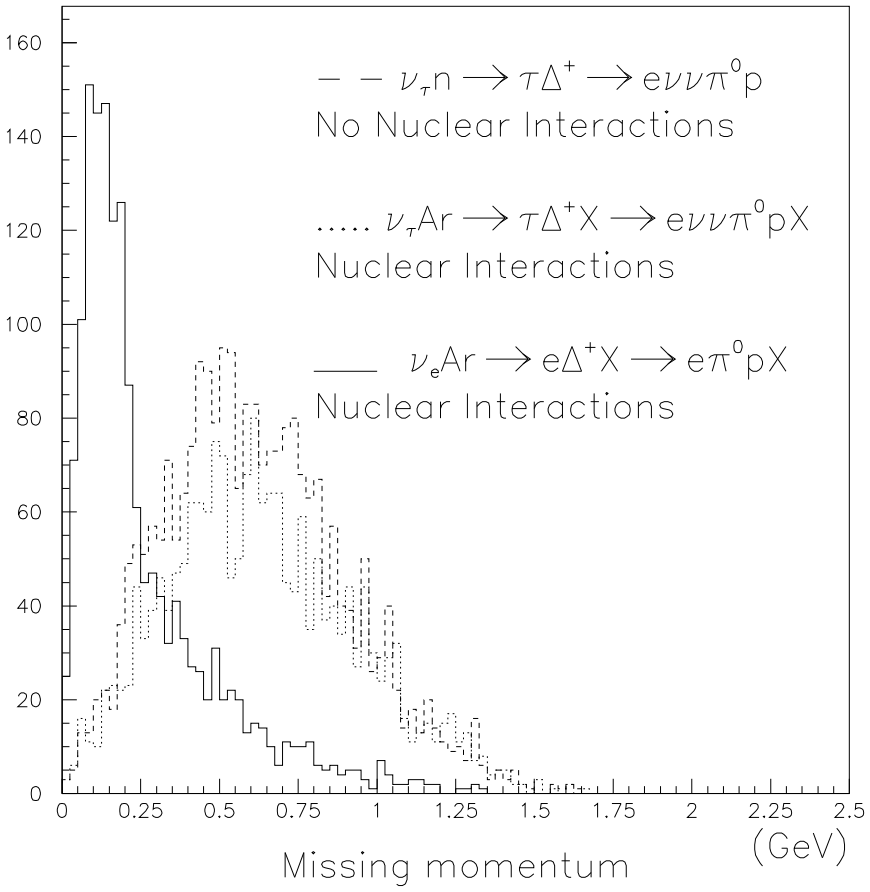

Figure 16: *Missing momentum in ν_e bound nucleon $\Delta^+ \rightarrow p\pi^0$ interactions (full line); in ν_τ free nucleon interactions (dashed line); in ν_τ bound nucleon interactions (dotted line)*

Proc. of the *Specialists' Meeting on Shielding Aspects of Accelerators, Targets & Irradiation Facilities*, Arlington, April 28-29 1994, (published by OECD/NEA 1995), p. 287; A. Fassò, A. Ferrari, J. Ranft, and P. R. Sala, in *Intermediate Energy Nuclear Data: Models and codes*, Proc. of a specialist' meeting, Issy-les-Moulineaux, May 30th - June 1st 1994, (published by OECD/NEA 1994), p. 271.

[4] A. Fassò, A. Ferrari, J. Ranft and P. R. Sala, Proc. of the 2nd workshop on *Simulating Accelerator Radiation Environment, SARE2*, CERN-Geneva, October 9–11 1995, CERN Divisional report CERN/TIS-RP/97-05 (1997), p. 158.

[5] A. Ferrari, and P. R. Sala, Proc. of the *Workshop on Nuclear Reaction Data and Nuclear Reactors Physics, Design and Safety*, International Centre for Theoretical Physics, Miramare–Trieste, Italy, 15 April – 17 May 1996 in press

[6] A. Rubbia, private communication

[7] E. Gadioli, and P.E. Hodgson, *Pre-equilibrium Nuclear Reactions*, (Clarendon Press, Oxford, 1992).

[8] J. J. Griffin, *Phys. Rev. Lett.* 17, 438 (1966).

[9] V.F. Weisskopf, *Phys. Rev.* 52, 295 (1937).

[10] A. Ferrari, P.R. Sala, J. Ranft, and S. Roesler, *Z. Phys.* C70, 413 (1996).

[11] E. Fermi, *Prog. Theor. Phys.* 5, 1570 (1950).

[12] M. Epherre and E. Gradsztajn, *J. Physique* 18, 48 (1967.

[13] A. Ferrari, P.R. Sala, J. Ranft, and S. Roesler, *Z. Phys.* C71, 75 (1996).

[14] M.E. Grypeos, G.A. Lalazissis, S.E. Massen and C.P. Panos, *J. Phys.* G17, 1093 (1991).

[15] L.R.B. Elton, *Nuclear Sizes*, (Oxford University Press, Oxford 1961).

[16] W.D. Myers, *Nucl. Phys.* A204, 465 (1973).

[17] W.D. Myers, *Droplet Model of Atomic Nuclei*, (IFI/Plenum Data Company, New York 1977).

[18] C. Ciofi degli Atti and S. Simula, *Phys. Rev.* C53 1689 (1996).

[19] P. Fernandez de Cordoba et al., *Nucl. Phys.* A611 514 (1996).

[20] K. Hänssgen, and J. Ranft, *Nucl. Sci. Eng.* 88, 537 (1984).

[21] Phase shift solutions KH78, KH80, in *Landolt-Börnstein , new series* , Vol. 9, part II, (Springer-Verlag 1983).

[22] J.N. Ginocchio, *Phys. Rev.* C17, 195 (1978).

[23] E. Oset, and L.L. Salcedo, *Nucl. Phys.* A468, 631 (1987).

[24] T. Ericson and W. Weise, *Pions and Nuclei*, (Clarendon Press, Oxford, 1988).

[25] M.J. Vicente Vacas, and E. Oset, *Nucl. Phys.* A568, 855 (1994).

[26] L. Stodolski, Proc. of the *Vth Intern. Coll. on Multiparticle Reactions*, Oxford, 577 (1975).

[27] L. Landau, I. Pomeranchuk, *Dokl. Akad. Nauk SSSR* 92, 535 (1953); A.B. Migdal, *Phys. Rev.* 103, 1811 (1956).

[28] A. Bohr, B.R. Mottelson, *Nuclear Structure* Vol. 1, (W.A. Benjamin, Inc. 1969).

[29] M. Blann, *Phys. Rev. Lett.* 27, 337 (1971).

[30] M. Blann, *Phys. Rev. Lett.* 28, 757 (1972).

[31] M. Blann and H.K. Vonach, *Phys. Rev.* C28, 1475 (1983).

[32] M. Blann, *Phys. Rev.* C28, 1648 (1983).

[33] K. Kikuchi and M. Kawai, *Nuclear Matter and Nuclear Interactions*, (North-Holland, Amsterdam, 1968).

[34] M. Trabandt et al., *Phys. Rev.* C39, 452 (1989).

[35] A.A. Cowley et al., *Phys. Rev.* C43, 678 (1991).

[36] K. Ishibashi et al., *J. Nucl. Sci. Technol.* 32, 827 (1995).

[37] W.B. Amian et al., *Nucl. Sci. Eng.* 115, 1 (1993).

[38] S.M. Levenson et al., *Phys. Rev.* C28, 326 (1983).

[39] D. Ashery et al., *Phys. Rev.* C30, 946 (1984).

[40] A. Leprêtre et al., *Nucl. Phys.* A390, 221 (1982)

[41] K.Nakai et. al., *Phys. Rev. Lett.* 44, 1446 (1979).

[42] D. Ashery et al., *Phys. Rev.* C23, 2173 (1981).

[43] G. Mantzouranis, D. Agassi, and H. A. Weidenmüller, *Phys. Lett.* 57B, 220 (1975).

[44] J. M. Akkermans, H. Gruppelaar and G. Reffo, *Phys. Rev.* C22, 73 (1980).